
CLOSING THE LOOP: A CONTROL-THEORETIC FRAMEWORK FOR PROVABLY STABLE TIME SERIES FORECASTING WITH LLMs

Xingyu Zhang, Hanyun Du, Zeen Song, Jianqi Zhang

University of Chinese Academy of Sciences

Beijing, China

{Zhangxingyu23, Duhanyun25, Songzeen22, Zhangjianqi23}@mails.ucas.ac.cn

Changwen Zheng, Wenwen Qiang

Institute of Software, Chinese Academy of Sciences

Beijing, China

{Changwen, qiangwenwen}@iscas.ac.cn

ABSTRACT

Large Language Models (LLMs) have recently shown exceptional potential in time series forecasting, leveraging their inherent sequential reasoning capabilities to model complex temporal dynamics. However, existing approaches typically employ a naive autoregressive generation strategy. We identify a critical theoretical flaw in this paradigm: during inference, the model operates in an open-loop manner, consuming its own generated outputs recursively. This leads to inevitable error accumulation (exposure bias), where minor early deviations cascade into significant trajectory drift over long horizons. In this paper, we reformulate autoregressive forecasting through the lens of control theory, proposing **F-LLM** (Feedback-driven LLM), a novel closed-loop framework. Unlike standard methods that passively propagate errors, F-LLM actively stabilizes the trajectory via a learnable residual estimator (Observer) and a feedback controller. Furthermore, we provide a theoretical guarantee that our closed-loop mechanism ensures uniformly bounded error, provided the base model satisfies a local Lipschitz constraint. Extensive experiments demonstrate that F-LLM significantly mitigates error propagation, achieving good performance on time series benchmarks.

1 Introduction

Time Series Forecasting (TSF) stands as a pivotal component in modern data-driven decision-making, underpinning critical applications ranging from energy grid management [12, 13] to extreme weather event prediction [14, 16]. While recent deep learning approaches, such as DLinear [50] and PatchTST [44], have achieved significant strides by learning mapping functions in a supervised manner, they primarily function as discriminative regressors. These methods often approximate the conditional expectation of future values, which tends to yield over-smoothed predictions [5] and struggles to capture the intrinsic stochasticity and complex, multi-modal dependencies inherent in long-horizon trajectories [6].

To address these limitations, a paradigm shift has emerged with the adaptation of Large Language Models (LLMs) for time series analysis [149]. By treating continuous time series data as a sequence of continuous tokens, these foundation models leverage their immense pre-trained knowledge to perform generative forecasting. Unlike traditional regression, autoregressive LLMs model the joint probability distribution of the future sequence as Fig.1(a). This capability allows them to preserve temporal coherence, capture long-range dependencies, and exhibit remarkable zero-shot generalization potential across diverse domains.

However, the direct application of the linguistic “next-token prediction” paradigm to continuous dynamics introduces a fundamental structural vulnerability: **Error Accumulation**. Standard LLMs are trained under a “Teacher Forcing” regime, where the model is conditioned on ground-truth history. Yet, during inference, the model operates in an open-loop autoregressive mode, consuming its own generated outputs recursively to predict subsequent steps. This

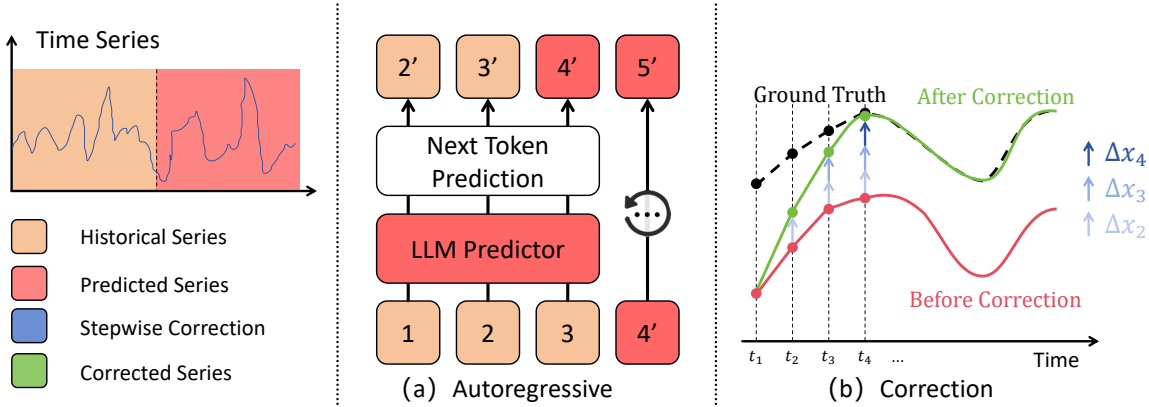


Figure 1: Comparison of standard autoregressive generation and the proposed stepwise correction strategy. (a) Standard autoregressive LLMs suffer from cumulative prediction drift, where minor deviations at each step are fed back as input, causing errors to accumulate over time. (b) The stepwise correction strategy intervenes in this process by adjusting the prediction at each step before it enters the next autoregressive loop, thereby preventing error propagation and stabilizing the trajectory.

discrepancy creates a distribution shift known as **Exposure Bias** [2]. In the continuous domain, even a microscopic error ϵ at step t introduces a covariate shift for step $t + 1$. Without ground-truth correction as Fig.1(b), these errors do not cancel out; instead, they propagate and amplify through the feedback loop, exhibiting compound growth [4]. This “snowball effect” causes the predicted trajectory to drift irreversibly away from the true data manifold as the forecasting horizon extends, rendering naive autoregressive LLMs unreliable for long-term tasks.

In this paper, we argue that addressing this instability requires more than just scaling model size; it necessitates a fundamental reformulation of the inference process from an open-loop generation to a **closed-loop control system**. Drawing inspiration from classical control theory, we propose **F-LLM** (Feedback-driven LLM). Our core insight is to view the forecasting error not merely as a performance metric, but as a state disturbance that must be actively rejected. Since the true error is unobservable during inference (due to the absence of ground truth), we introduce a learnable **Residual Estimator** that functions as a system **Observer**, inferring the latent error state from the current context. This estimate is then fed into a **Feedback Controller** to calibrate the trajectory on-the-fly. To ensure mathematical stability, we explicitly impose a Local Lipschitz constraint, guaranteeing that the error dynamics remain within a controllable regime amenable to linear feedback.

Our work makes the following contributions: **1)** We provide a rigorous analysis of the error propagation mechanism in autoregressive LLMs, demonstrating that standard open-loop inference inherently suffers from exponential error divergence due to unbounded spectral properties; **2)** We propose F-LLM, a novel framework that seamlessly integrates deep generative models with closed-loop feedback control. This is the first work to successfully apply dynamic error correction to stabilize LLM-based forecasting; **3)** Beyond empirical design, we provide a mathematical proof that our closed-loop mechanism guarantees uniformly bounded prediction error under mild assumptions, offering a theoretical safety assurance often missing in deep learning methods; **4)** Extensive experiments on widely benchmarks demonstrate that F-LLM significantly mitigates trajectory drift, achieving superior performance in long-term forecasting tasks.

2 Related Works

With the advent of deep learning [70], the field of TSF has witnessed a transition from statistical methods to data-driven neural architectures. These approaches can be broadly categorized based on their core mechanisms: RNN-based models [29, 39] capture sequential dependencies; CNN-based methods [38, 28] extract local temporal features; and MLP-based architectures [94, 50] emphasize efficient point-wise mapping. Recently, Transformer-based models have dominated the landscape, focusing on different modeling perspectives: temporal-domain methods like PatchTST [44] and TimesNet [42] capture multi-scale dependencies; frequency-domain approaches such as FEDFormer [49] utilize Fourier or Wavelet transforms for global modeling; and cross-variable methods like iTransformer [27] explicitly model multivariate correlations. Despite their success, these models operate primarily as discriminative regressors, typically requiring extensive training on domain-specific data, which limits their zero-shot generalization capabilities across diverse scenarios.

Recognizing the generalization power of foundation models, recent research explores adapting LLMs for TSF through two distinct paradigms. The first stream treats the LLM primarily as a deep feature extractor followed by a global projection head. Methods such as FPT [144], Time-LLM [146], and PromptCast [142], reprogram the input time series into text-aligned prototypes or embeddings, but eventually rely on a linear layer to predict the entire future horizon in a single forward pass. While this avoids error accumulation, it fundamentally reduces the generative LLM to a discriminative regressor, failing to fully exploit the model’s intrinsic capacity for sequential reasoning and probabilistic modeling. To better align with the LLM’s pre-training objective, a second stream advocates for autoregressive generation, represented by LLMTIME [143] and AutoTimes [149]. By staying faithful to the “next-token” paradigm, these methods model the joint probability of the future sequence, thereby capturing complex temporal dependencies. However, a critical limitation persists across these autoregressive generation methods: they rely on naive autoregressive generation. This open-loop process, which recursively consumes generated outputs, lacks a correction mechanism for the inevitable prediction errors, rendering long-term forecasts prone to trajectory divergence.

The discrepancy between teacher-forced training and free-running inference, known as exposure bias, is a classical challenge in sequence generation [2]. Traditional mitigation strategies, such as Scheduled Sampling [2] or sequence-level optimization [158], require intervening in the training process. For LLM-based forecasting, however, retraining is often computationally prohibitive or infeasible due to restricted access to model weights. Consequently, inference-time solutions are preferred. While simple heuristic adjustments exist, they fail to address the fundamental dynamics of error accumulation in continuous time series. This highlights a significant gap in the literature: in the context of TSF, lack of a rigorous, control-theoretic framework that can stabilize the autoregressive generation of frozen LLMs without necessitating expensive retraining.

3 Notation and Problem Formulation

We begin by establishing the mathematical foundations of TSF and the autoregressive paradigm of LLMs, identifying a theoretical gap when applying the latter to the former.

TSF via Autoregression. Let $x_{1:T} \in \mathbb{R}^{T \times D}$ denote a multivariate historical time series of length T with D variables. The objective is to predict the future horizon $x_{T+1:T+H} \in \mathbb{R}^{H \times D}$. While traditional methods often model this as a direct mapping $f: \mathbb{R}^{T \times D} \rightarrow \mathbb{R}^{H \times D}$, LLMs operate on a generative paradigm. An LLM, parameterized by θ , functions as a probabilistic predictor g_θ that models the joint distribution of the future sequence via the chain rule. Specifically, the probability of the future trajectory is factorized as:

$$P(x_{T+1:T+H} \mid x_{1:T}) = \prod_{k=1}^H P(x_{T+k} \mid x_{1:T}, x_{T+1:T+k-1}). \quad (1)$$

Eq.1 aligns with the pre-training objective of maximizing the conditional likelihood of the next token, thereby effectively leveraging the model’s inductive biases for sequential reasoning and zero-shot generalization [149].

The Open-Loop Vulnerability Despite the representational advantages of this paradigm, the recursive nature of inference introduces a structural vulnerability known as error accumulation. During the forecasting phase, the model operates in an open loop where the prediction at step $t+k$ relies on the estimate \hat{x}_{t+k-1} rather than the ground truth. Formally, the recursive generation is defined as:

$$\hat{x}_{t+k} = g_\theta(\hat{X}_{t+k-1}), \quad (2)$$

where the context \hat{X}_{t+k-1} comprises historical input and previously generated outputs. This creates a discrepancy between the teacher-forced training distribution and the autoregressive inference distribution, a phenomenon widely recognized in sequence generation literature as exposure bias [2, 3]. Such discrepancy induces covariate shift [164], allowing early prediction errors to propagate through the feedback loop. In the context of continuous dynamics, this leads to compound growth of the error norm over the horizon [4]. Consequently, we posit that robust long-term forecasting cannot be achieved by simple recursive generation alone but requires reformulating the inference process as a stabilized control system with active error correction.

4 Theoretical Analysis

In this section, we scrutinize the error propagation mechanism in autoregressive forecasting. We demonstrate that standard open-loop generation inherently suffers from exponential error growth and rigorously derive the conditions required to achieve bounded stability through closed-loop feedback.

4.1 Open-Loop Error Dynamics

Let $\Delta x_t = \hat{x}_t - x_t$ denote the prediction error at step t . We assume the underlying ground truth process follows a dynamic system $x_t = f(x_{t-1}) + w_t$, where w_t represents the inherent stochasticity. In the standard autoregressive setting, the predictor g_θ consumes its own previous output. By linearizing the predictor around the data manifold using a first-order Taylor expansion, the error evolution can be approximated as:

$$\Delta x_t \approx J_g(x_{t-1})\Delta x_{t-1} + \epsilon_t. \quad (3)$$

Here, $J_g(x) = \partial g_\theta(x)/\partial x$ is the local Jacobian matrix representing the model's sensitivity to input perturbations, and ϵ_t encapsulates the single-step modeling error and noise.

The stability of this dynamical system is governed by the spectral properties of the transition operator J_g . Standard training objectives such as maximum likelihood estimation do not enforce contractive constraints. Moreover, to capture long-term dependencies and mitigate the vanishing gradient problem during training, optimization algorithms often drive the model parameters into a regime where the spectral radius $\rho(J_g)$ is close to or exceeds unity [8]. Without explicit regularization [9], high-capacity models typically exhibit $\rho(J_g) > 1$ in local regions. Consequently, the expected error norm tends to grow exponentially with the forecast horizon H :

$$\mathbb{E}[\|\Delta x_{t+H}\|] \sim \mathcal{O}(\rho(J_g)^H), \quad (4)$$

leading to inevitable trajectory divergence. To formalize the error growth, we present the following proposition derived from the linearized dynamics.

Proposition 4.1 (Exponential Error Growth) *Consider the linearized error dynamics $\Delta x_{t+1} \approx J_g \Delta x_t + \epsilon_t$. If the spectral radius $\rho(J_g) > 1$, the upper bound of the expected error norm grows exponentially with the horizon H .*

The proof of the above proposition is presented in Appendix C. This derivation highlights that simply reducing the single-step error ϵ_t is insufficient for long-term stability if the underlying operator is expansive ($\rho(J_g) > 1$).

4.2 Closed-Loop Stabilization

To mitigate the above divergence, we propose altering the error dynamics by introducing a linear feedback correction term. Specifically, we adjust the prediction by injecting a correction signal proportional to the previous error, denoted as:

$$\hat{x}_t^{\text{closed}} = g_\theta(\hat{X}_{t-1}) - L\Delta x_{t-1}, \quad (5)$$

where $L \in \mathbb{R}^{D \times D}$ is a learnable feedback gain matrix. Substituting this into the error equation transforms the system into a closed-loop form, approximated as:

$$\Delta x_t^{\text{closed}} \approx (J_g(x_{t-1}) - L)\Delta x_{t-1} + \epsilon_t. \quad (6)$$

The effective transition operator is now shifted from J_g to $(J_g - L)$. The objective of robust forecasting thus reduces to a control problem: finding a gain L that renders the closed-loop operator contractive.

4.3 Stability Guarantee

We now provide a theoretical guarantee that such a feedback mechanism ensures long-term robustness.

Theorem 4.1 (Bounded Stability via Feedback) *Assume the single-step modeling error is bounded, i.e., $\|\epsilon_t\| \leq \gamma$ for some finite γ . If there exists a feedback gain L and a constant $q \in [0, 1)$ such that the closed-loop operator satisfies the contraction condition $\|J_g(x) - L\|_2 \leq q$ for all x , then the cumulative error sequence is uniformly bounded:*

$$\limsup_{t \rightarrow \infty} \|\Delta x_t\| \leq \frac{\gamma}{1 - q}. \quad (7)$$

Before presenting the proof, we justify the validity of the assumptions. First, the bounded error assumption is standard in statistical learning theory [7] and is practically satisfied in our setting because modern Transformer architectures employ normalization layers (e.g., LayerNorm) and bounded activation functions, which inherently constrain the magnitude of the output features. Second, the existence of a stabilizing gain L (the contraction condition) is not guaranteed for arbitrary neural networks but is explicitly promoted by the Local Lipschitz Regularization, which constrains the spectral radius of the underlying Jacobian to be amenable to linear feedback control. Finally, the proof of the above theorem is shown in Appendix D.

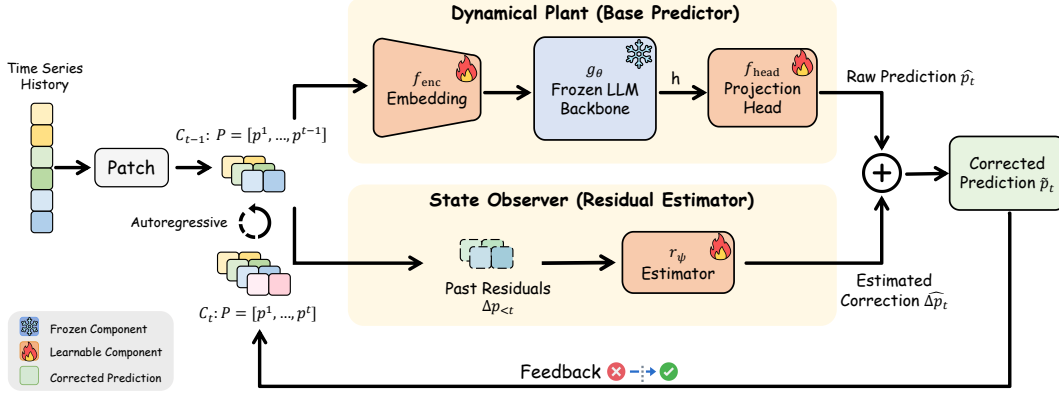


Figure 2: The overall framework of F-LLM. The system operates as a closed-loop control mechanism where a frozen LLM as the Plant generates raw predictions, while a lightweight Residual Estimator as the Observer predicts trajectory deviations based on historical errors. The estimated residuals are injected back into the context via an in-loop correction mechanism to mitigate error accumulation.

4.4 Deriving the Architecture from Theory

Theorem 4.1 serves as more than a theoretical proof; it acts as a blueprint for our architectural design. The theorem explicitly requires two conditions to hold, which directly map to the novel components of our proposed framework.

First, the feedback mechanism mathematically requires access to the previous error Δx_{t-1} . However, during inference, the ground truth x_{t-1} is unavailable, making the error state unobservable. This theoretical constraint necessitates the introduction of a Residual Estimator to approximate the latent error state, acting as an observer in the control loop.

Second, for the condition $\|J_g - L\|_2 \leq q < 1$ to be feasible via a linear gain L , the raw Jacobian J_g must be bounded and well-conditioned. If the base model g_θ is arbitrarily chaotic, no stabilizing L exists. This controllability requirement mandates the imposition of a Local Lipschitz Regularization on the base predictor during training, constraining the sensitivity of g_θ to ensure it remains within a controllable regime.

5 Methodology

Guided by the theoretical constraints derived in Section 4, we instantiate our framework, **F-LLM** (Feedback-driven LLM). As illustrated in Figure 2, F-LLM instantiates a closed-loop control loop composed of three modules: a base predictor acting as the dynamical plant, a residual estimator acting as the state observer, and a feedback mechanism acting as the controller. Furthermore, we introduce a two-stage curriculum to ensure stable optimization of these components.

5.1 The F-LLM Architecture

Patch-wise Autoregressive Predictor To align the continuous time series with the semantic space of LLMs, we adopt a patch-based formulation. Given a historical sequence $x \in \mathbb{R}^T$, we segment it into non-overlapping patches $P = [p_1, \dots, p_N]$, where each $p_i \in \mathbb{R}^L$. The base predictor, denoted as the ‘‘Plant’’, consists of a learnable embedding layer f_{enc} to project patches into the LLM’s embedding space, a frozen LLM backbone g_θ predict in the embedding space, and a learnable inverse embedding layer f_{head} project back time series space. At step t , the plant generates a raw prediction based on the context \mathcal{C}_{t-1} :

$$\hat{p}_t = f_{\text{head}}(g_\theta(f_{\text{enc}}(\mathcal{C}_{t-1}))). \quad (8)$$

Residual Estimator Since the true error Δp_t is unobservable during predict, we employ a Residual Estimator r_ψ to act as the system observer. This lightweight network takes the sequence of past estimated residuals $\Delta P_{<t}$ as input and predicts the correction term for the current step:

$$\hat{\Delta p}_t = r_\psi(\Delta P_{<t}). \quad (9)$$

Mathematically, r_ψ parameterizes the optimal control law derived in Eq.(6), learning to predict the trajectory deviation required to reject disturbances.

Closed-Loop Interaction The feedback loop is closed by injecting the estimated residual into the prediction. The final corrected patch is:

$$\tilde{p}_t = \hat{p}_t + \hat{\Delta p}_t. \quad (10)$$

Unlike post-hoc correction methods, F-LLM is an in-loop framework: the corrected patch \tilde{p}_t is appended to the context C_t for the next autoregressive step. This prevents the “snowball effect” described in Section 4 by constantly recalibrating the generative trajectory back to the data manifold.

5.2 Two-Stage Curriculum Learning

Jointly optimizing the Plant and the Observer is unstable due to the “moving target” problem: initial random projections produce unstructured noise that confuses the estimator. To decouple representation alignment from control learning, we adopt a two-stage strategy.

Stage 1: Open-Loop Alignment First, we freeze the Residual Estimator and train only the projection layers ($f_{\text{enc}}, f_{\text{head}}$). We utilize Teacher Forcing, conditioning the model on ground-truth history to stabilize the feature alignment. To satisfy the controllability condition in Theorem 4.1 without computationally expensive regularization on the entire LLM, we impose a Local Lipschitz constraint on the actuator f_{head} . Specifically, we perturb the latent output h with a noise vector δ ($\|\delta\|_2 < \xi$, where ξ denotes the local neighborhood radius) and penalize the amplification of the output difference:

$$\mathcal{L}_{\text{lip}} = \mathbb{E}_{h, \delta} \left[\left(\frac{\|f_{\text{head}}(h + \delta) - f_{\text{head}}(h)\|_2}{\|\delta\|_2} - \kappa \right)_+^2 \right], \quad (11)$$

where κ is a hyperparameter controlling the desired Lipschitz constant. The objective is the standard reconstruction loss combined with the Lipschitz constraint:

$$\mathcal{L}_1 = \frac{1}{N} \sum_t \|p_t - \hat{p}_t\|_2 + \lambda \mathcal{L}_{\text{lip}}, \quad (12)$$

where λ is a hyperparameter. This stage ensures the Plant behaves as a robust dynamical system with bounded sensitivity.

Stage 2: Closed-Loop Feedback Learning Once the plant stabilizes, we freeze the projection layers and activate the Residual Estimator r_{ψ} . In this stage, we switch to a Closed-Loop regime, which approximates student forcing. The model generates the next step \hat{p}_t , calculates the residual $\Delta p_t = p_t - \hat{p}_t$ using the ground truth p_t (available during training), and supervises the estimator to predict this deviation. Specifically, we optimize r_{ψ} to minimize the estimation error:

$$\mathcal{L}_2 = \frac{1}{N} \sum_t \|(p_t - \hat{p}_t) - r_{\psi}(\hat{\Delta p}_{t-1})\|_2. \quad (13)$$

By learning to capture systematic bias of frozen plant, r_{ψ} effectively enables precise error cancellation during inference.

6 Experiments

We conduct extensive experiments to evaluate the effectiveness of F-LLM from multiple perspectives. Specifically, we aim to answer the following questions: (1) whether in-loop residual feedback improves long-horizon forecasting accuracy under standard supervised settings; (2) whether such correction preserves the zero-shot generalization ability of frozen LLM forecasters; and (3) how robust and efficient the proposed framework is across different datasets, LLM backbones, and hyperparameter choices.

6.1 Time Series Forecasting

Experimental Setup. We evaluate F-LLM on seven real-world multivariate time series datasets from the electricity, weather, and economy domains (Details in Appendix B). Hyperparameters such as learning rate, batch size, and hidden dimension are selected from pre-defined grids based on performance. We comprehensively compare F-LLM with representative forecasting models under standard settings in [149], where the lookback length is fixed to 672 and prediction horizons are $\{96, 192, 336, 720\}$. Baselines include conventional deep learning baselines (PatchTST [44], DLinear [50], Fedformer [49], TimesNet [42], SimpleTM [168], TimeMixer++ [169] and iTransformer [27]) to recent LLM-based approaches (TIME-LLM [146], AutoTimes [149], UniTime [145], LVICL [167], and FPT [144]).

Dataset	F-LLM		AutoTimes		LVICL		TimeLLM		FPT		Unitime		iTransformer		DLinear		PatchTST		TimesNet		TimeMixer++		SimpleTM	
	MSE	MAE	MSE	MAE	MSE	MAE	MSE	MAE	MSE	MAE	MSE	MAE	MSE	MAE	MSE	MAE	MSE	MAE	MSE	MAE	MSE	MAE	MSE	MAE
ETTh1	0.376	0.405	0.389	0.422	0.381	0.412	0.408	0.424	0.428	0.426	0.442	0.448	0.438	0.450	0.423	0.437	0.413	0.430	0.488	0.452	0.411	0.421	0.403	0.410
ETTh2	0.317	0.367	0.352	0.395	0.326	0.376	0.354	0.393	0.353	0.391	0.356	0.399	0.382	0.414	0.431	0.447	0.330	0.379	0.414	0.427	0.333	0.371	0.338	0.374
ETTm1	0.319	0.367	0.332	0.380	0.328	0.378	0.350	0.378	0.366	0.382	0.375	0.403	0.370	0.399	0.357	0.379	0.351	0.381	0.400	0.406	0.360	0.369	0.363	0.378
ETTm2	0.234	0.300	0.243	0.310	0.239	0.306	0.254	0.314	0.265	0.315	0.277	0.329	0.272	0.311	0.267	0.334	0.255	0.315	0.291	0.333	0.264	0.313	0.264	0.308
ECL	0.148	0.240	0.159	0.253	0.158	0.248	0.159	0.253	0.167	0.263	0.216	0.304	0.177	0.268	0.177	0.274	0.159	0.253	0.193	0.295	0.161	0.248	0.158	0.248
Weather	0.215	0.251	0.235	0.273	0.222	0.262	0.225	0.258	0.236	0.271	0.248	0.275	0.238	0.273	0.240	0.300	0.225	0.264	0.259	0.286	0.220	0.256	0.236	0.265
Traffic	0.364	0.261	0.374	0.264	0.370	0.260	0.388	0.264	0.414	0.294	0.429	0.304	0.379	0.272	0.434	0.295	0.391	0.264	0.620	0.329	0.409	0.260	0.422	0.276

Table 1: Long-term forecasting results averaged from four prediction lengths $\in \{96, 192, 336, 720\}$. Detailed results are in Appendix E. Most results of other methods derive from [149] and [167]. Results not reported are obtained by running each method’s source code; the look-back window is selected from $\{96, 336, 512, 672\}$ to report the best results.

Comparison Results. As Table 1 shows, across the five datasets, F-LLM achieves the best performance in most horizons. Compared with the strongest baseline on each setting (including both LLM4TS and non-LLM models), it reduces MSE by 5.6% on the most challenging long-horizon cases. Notably, these gains are obtained by adding a lightweight feedback module on top of frozen LLM forecasters, without modifying or retraining the backbone models.

6.2 Zero-Shot Forecasting

Large language models exhibit remarkable zero-shot generalization [151]. To assess whether this property transfers to TSF, we evaluate F-LLM in a zero-shot setting, where no samples from the target domain are used during training. Following the benchmark protocol of AutoTimes [149], a model is trained on a source dataset and applied to an unseen target domain without fine-tuning.

Experimental Setup. We conduct transfer learning between the M3 and M4 competition datasets, both rich in temporal variation but differing in statistical distribution. F-LLM is compared with representative LLM4TS forecasters, AutoTimes, and FPT. Each experiment includes a source–target pair (e.g., M4 Monthly \rightarrow M3 Monthly). For M4 \rightarrow M3, models trained on M4 Yearly, Quarterly, and Monthly subsets are evaluated on their M3 counterparts, while M3 Others uses the M4 Quarterly model to align forecast horizons. For M3 \rightarrow M4, the process is symmetric: M4 Yearly, Quarterly, and Monthly subsets use corresponding M3 models, and the remaining subsets (M4 Weekly, Daily, Hourly) adopt the model trained on M3 Monthly.

Comparison Results. As shown in Table 2, F-LLM attains the lowest SMAPE on 7 out of 8 transfer settings and is second best on the remaining one (M4 \rightarrow M3 Others, where FPT is slightly better). It consistently outperforms or matches both LLM-based forecasters (AutoTimes, FPT) and strong deep TSF baselines (e.g., DLinear and Transformer variants), indicating that the proposed bias correction module preserves the zero-shot generalization ability of LLMs while further improving cross-domain forecasting accuracy.

6.3 Ablation and Extended Analysis

We further conduct a series of ablation and sensitivity experiments to analyze the effectiveness, generality, and efficiency of the proposed F-LLM framework.

Effectiveness of each module. To assess the contribution of each component in F-LLM, we compare three variants: (1) F-LLM w/o Feedback: removing the bias correction module, (2) F-LLM w/o LLM: replacing the LLM forecaster with an MLP, and (3) F-LLM (Full): the complete model. As shown in Table 3, eliminating either component consistently degrades performance across all horizons on both ETTh1 and Weather datasets. The gap between the “F-LLM w/o Feedback” and “F-LLM (Full)” settings can also be interpreted as a concrete measure of the systematic bias between the original LLM forecasts and the ground truth, and the extent to which F-LLM reduces this mismatch. Figure 3 further visualizes 96-step forecasts, where the uncorrected LLM output exhibits gradual drift from the ground truth, whereas F-LLM adaptively offsets these deviations.

Generality Analysis. Previous LLM4TS studies [144, 146] have primarily designed their methods for specific LLM architectures, limiting their applicability to other models. In contrast, F-LLM is model-agnostic and can be seamlessly integrated with any decoder-only LLM. To demonstrate this flexibility, we implement F-LLM using several representative LLM backbones, including GPT-2 [153], OPT [152], and LLaMA [150]. As summarized in Table 4, the results show consistent performance gains across all backbones, confirming that the proposed bias correction strategy does not rely on a specific LLM architecture and generalizes consistently across different backbones.

Method	F-LLM	AutoTimes	FPT	DLinear	PatchTST	TimesNet	NSformer	FEDformer	Informer	Reformer	
M3 \rightarrow M4	Yearly	15.22	15.71	16.42	17.43	15.99	18.75	17.05	16.00	19.70	16.03
	Quarterly	9.06	9.35	10.13	9.74	9.62	12.26	12.56	9.48	13.00	9.76
	Monthly	13.68	14.06	14.10	15.65	14.71	14.01	16.82	15.12	15.91	14.80
	Others	5.08	5.79	4.81	6.81	9.44	6.88	8.13	8.94	13.03	7.53
M4 \rightarrow M3	Yearly	13.701	13.728	13.740	14.193	13.966	15.655	14.988	13.887	18.542	15.652
	Quarterly	10.723	10.742	10.787	18.856	10.929	11.877	11.686	11.513	16.907	11.051
	Monthly	14.535	14.558	14.630	14.765	14.664	16.165	16.098	18.154	23.454	15.604
	Others	6.245	6.259	7.081	9.194	7.087	6.863	6.977	7.529	7.348	7.001

Table 2: Results of zero-shot forecasting. We adopt the same protocol as FPT. M4 \rightarrow M3 means training forecasters on M4 datasets and evaluating the performance on M3, and vice versa. Lower SMAPE indicates better performance.

Dataset		ETTh1		Weather	
		MSE	MAE	MSE	MAE
Pred-96	F-LLM w/o Feedback	0.362	0.395	0.147	0.204
	F-LLM w/o LLM	0.377	0.406	0.149	0.215
	F-LLM (Full)	0.347	0.389	0.140	0.188
Pred-192	F-LLM w/o Feedback	0.390	0.415	0.203	0.254
	F-LLM w/o LLM	0.405	0.418	0.216	0.268
	F-LLM (Full)	0.375	0.402	0.185	0.231
Pred-336	F-LLM w/o Feedback	0.405	0.434	0.245	0.306
	F-LLM w/o LLM	0.416	0.443	0.255	0.311
	F-LLM (Full)	0.390	0.415	0.230	0.270
Pred-720	F-LLM w/o Feedback	0.417	0.444	0.320	0.341
	F-LLM w/o LLM	0.438	0.460	0.324	0.351
	F-LLM (Full)	0.395	0.427	0.305	0.318

Table 3: Ablation study on the effectiveness of individual components in F-LLM on the ETTh1 and Weather datasets.

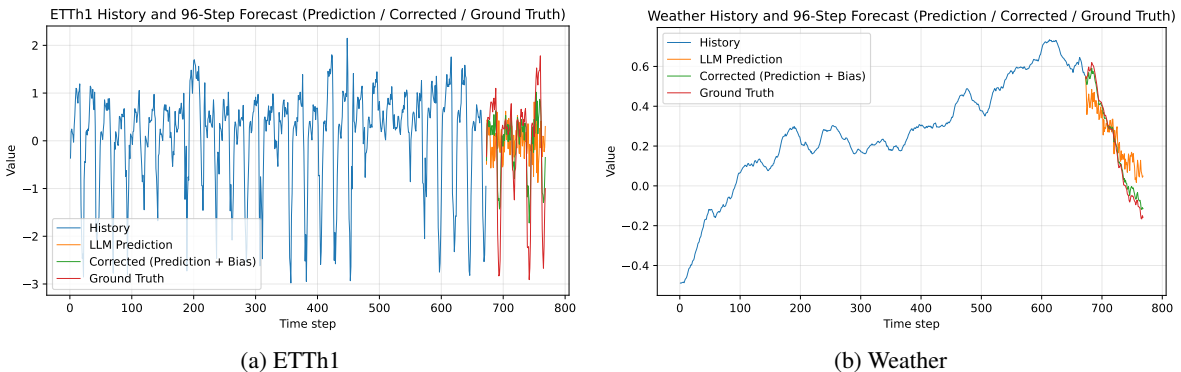


Figure 3: Comparison of 96-step forecasts on ETTh1 and Weather. The frozen LLM produces locally reasonable predictions but gradually accumulates stepwise errors along the autoregressive rollout. In contrast, F-LLM compensates for structured residual bias and maintains trajectory alignment over long horizons.

LLM	Metric	ETTh1				Traffic			
		96	192	336	720	96	192	336	720
GPT-2	MSE	0.352	0.382	0.399	0.420	0.361	0.381	0.397	0.440
	MAE	0.391	0.415	0.427	0.445	0.254	0.263	0.272	0.292
OPT-6.7B	MSE	0.351	0.381	0.394	0.418	0.353	0.364	0.389	0.424
	MAE	0.390	0.413	0.421	0.443	0.248	0.258	0.270	0.290
LLaMA	MSE	0.347	0.375	0.390	0.395	0.330	0.352	0.370	0.405
	MAE	0.379	0.402	0.415	0.427	0.242	0.250	0.272	0.281

Table 4: Performance of F-LLM with different frozen LLM backbones under a fixed context length $C = 672$. Consistent improvements across GPT-2 (124M), OPT, and LLaMA-7B demonstrate that the proposed residual feedback correction is model-agnostic and independent of the underlying LLM architecture.

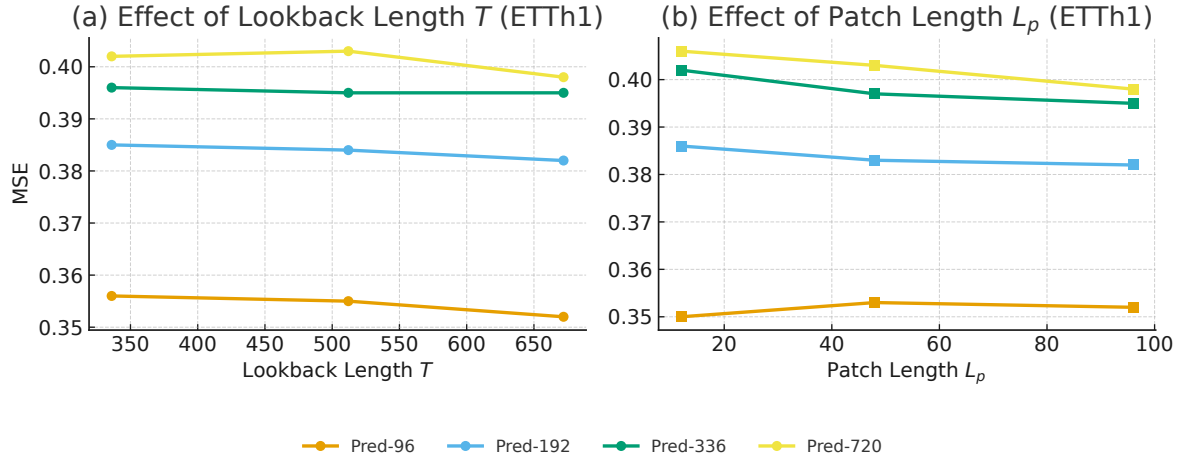


Figure 4: Sensitivity analysis of F-LLM to the historical lookback length T and patch length L_p on the ETTh1 dataset. The results show that F-LLM maintains stable performance across a wide range of hyperparameter choices, indicating that the observed gains are not sensitive to specific context-length or tokenization settings.

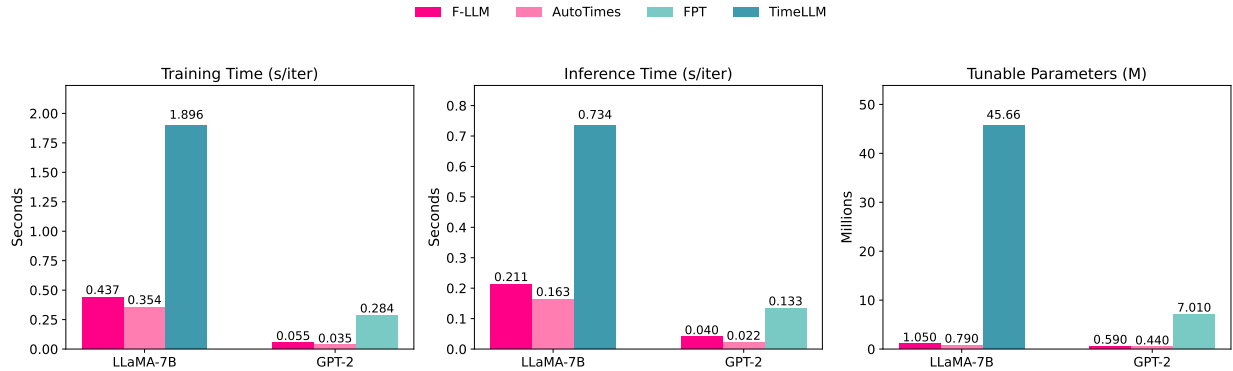


Figure 5: Efficiency comparison between F-LLM and representative LLM4TS methods in terms of training and inference time as well as the number of tunable parameters, measured with the same batch size (224) on the ETTh1 dataset. F-LLM introduces only marginal computational overhead by adding a lightweight inference-time feedback module on top of frozen LLM backbones.

Hyperparameter Sensitivity. We further investigate the sensitivity of F-LLM to two critical hyperparameters that influence forecasting accuracy: the historical lookback length T and the patch length L_p . Both parameters jointly determine the effective temporal range and tokenization granularity of the LLM-based forecaster. Specifically, we vary the lookback length $T \in \{336, 512, 672\}$ and the patch length $L_p \in \{12, 48, 96\}$ on the ETTh1 dataset, and report the corresponding MSE across four forecasting horizons. The results are summarized in Figure 4. As T increases, the model performance gradually improves and then stabilizes, indicating that extending the historical context benefits prediction up to a certain point. Regarding the patch length, moderate segment sizes (around $L_p = 48$) yield the most favorable results, while overly short or long patches slightly reduce accuracy. These observations suggest that F-LLM maintains stable performance under a range of hyperparameter choices, and that the patching design is not the main source of gains but mainly helps capture local temporal patterns before feeding them to the frozen LLM backbone.

Efficiency Analysis. We further evaluate the efficiency and robustness of F-LLM compared with representative LLM4TS baselines. As shown in Figure 5, F-LLM achieves comparable runtime efficiency to AutoTimes while introducing less than 5% additional inference time relative to the frozen LLM baseline under the same hardware and batch size settings. Although F-LLM contains slightly more tunable parameters than AutoTimes, its runtime is even shorter, which can be attributed to the absence of redundant contextual expansion. This efficiency is enabled by the minimal overhead of the feedback correction module, which consists of a single linear layer. Despite its lightweight design, F-LLM consistently improves forecasting accuracy with negligible computational cost. Furthermore, to

Dataset	ECL				ETTh1	
	Horizon		MSE	MAE	MSE	MAE
96			0.117±0.002	0.204±0.001	0.347±0.002	0.379±0.003
192			0.139±0.002	0.230±0.003	0.375±0.003	0.402±0.001
336			0.150±0.003	0.248±0.001	0.390±0.002	0.415±0.002
720			0.186±0.002	0.279±0.004	0.395±0.003	0.427±0.004

Table 5: Robustness evaluation of F-LLM on the ECL and ETTh1 datasets for input length is 672 and output length across $\{96, 192, 336, 720\}$. The reported mean and standard deviation over five independent runs demonstrate stable performance.

disentangle the effect of inference-time residual correction from parameter-efficient fine-tuning, we conduct a controlled comparison among three settings: (1) the frozen LLM baseline, (2) the frozen LLM baseline equipped with LoRA, and (3) F-LLM with residual feedback correction. As shown in Table 6, LoRA yields moderate improvements by adapting the LLM parameters during training, while F-LLM consistently achieves larger gains, especially in long-horizon forecasting. These results indicate that correcting structured prediction bias at inference time is more effective than lightweight parameter adaptation for mitigating error accumulation in autoregressive forecasting.

Dataset	Metric	ETTh1		ECL		Weather	
		MSE	MAE	MSE	MAE	MSE	MAE
Pred-96	Frozen LLM	0.362	0.395	0.142	0.235	0.147	0.204
	+ LoRA	0.358	0.395	0.131	0.221	0.145	0.195
	F-LLM	0.347	0.389	0.117	0.204	0.140	0.188
Pred-192	Frozen LLM	0.390	0.415	0.161	0.251	0.203	0.254
	+ LoRA	0.390	0.416	0.147	0.244	0.198	0.242
	F-LLM	0.375	0.402	0.139	0.230	0.185	0.231
Pred-336	Frozen LLM	0.405	0.434	0.174	0.269	0.245	0.306
	+ LoRA	0.406	0.434	0.168	0.255	0.238	0.291
	F-LLM	0.390	0.415	0.150	0.248	0.230	0.270
Pred-720	Frozen LLM	0.417	0.444	0.218	0.302	0.320	0.340
	+ LoRA	0.414	0.442	0.207	0.290	0.311	0.325
	F-LLM	0.395	0.427	0.186	0.279	0.305	0.318

Table 6: Comparison of long-term forecasting performance under different adaptation strategies. We compare the frozen LLM baseline, LLM equipped with LoRA, and F-LLM. All results are reported under the same experimental settings.

Robustness Analysis We evaluate the robustness of the proposed F-LLM. As shown in Table 5, across ECL and ETTh1 datasets and for all forecasting horizons, F-LLM exhibits consistently small variance, indicating stability to random initialization and stochastic training.

7 Conclusion

In this paper, we identified the structural vulnerability of Error Accumulation inherent in applying autoregressive Large Language Models to continuous time series forecasting. To mitigate the inevitable trajectory drift caused by open-loop inference, we proposed **F-LLM**, a novel framework that reformulates forecasting as a closed-loop control problem. By integrating a Residual Estimator as a system observer and enforcing Local Lipschitz constraints for controllability, F-LLM effectively rejects disturbances and actively calibrates the generative path. Our theoretical analysis provides a rigorous guarantee of uniformly bounded errors. Extensive experiments have confirmed that F-LLM achieves good performance in benchmark tests, while retaining the zero-shot generalization ability of frozen LLM.

References

- [1] Y. Bengio and Y. LeCun, “Scaling learning algorithms towards AI.” MIT Press, 2007.
- [2] S. Bengio, O. Vinyals, N. Jaitly, and N. Shazeer, “Scheduled sampling for sequence prediction with recurrent neural networks,” *Advances in neural information processing systems*, vol. 28, 2015.
- [3] M. Ranzato, S. Chopra, M. Auli, and W. Zaremba, “Sequence level training with recurrent neural networks,” *arXiv preprint arXiv:1511.06732*, 2015.
- [4] A. Venkatraman, M. Hebert, and J. Bagnell, “Improving multi-step prediction of learned time series models,” in *Proceedings of the AAAI Conference on Artificial Intelligence*, vol. 29, no. 1, 2015.

- [5] M. Mathieu, C. Couarie, and Y. LeCun, “Deep multi-scale video prediction beyond mean square error,” *arXiv preprint arXiv:1511.05440*, 2015.
- [6] K. Rasul, C. Seward, I. Schuster, and R. Vollgraf, “Autoregressive denoising diffusion models for multivariate probabilistic time series forecasting,” in *International Conference on Machine Learning*. PMLR, 2021, pp. 8857–8868.
- [7] M. Mohri, A. Rostamizadeh, and A. Talwalkar, *Foundations of machine learning*. MIT press, 2018.
- [8] R. Pascanu, T. Mikolov, and Y. Bengio, “On the difficulty of training recurrent neural networks,” in *International conference on machine learning*. PMLR, 2013, pp. 1310–1318.
- [9] J. Sokolic, R. Giryes, G. Sapiro, and M. R. Rodrigues, “Robust large margin deep neural networks,” in *Artificial Intelligence and Statistics*. PMLR, 2017, pp. 1495–1503.
- [10] G. E. Hinton, S. Osindero, and Y. W. Teh, “A fast learning algorithm for deep belief nets,” *Neural Computation*, vol. 18, pp. 1527–1554, 2006.
- [11] I. Goodfellow, Y. Bengio, A. Courville, and Y. Bengio, *Deep learning*. MIT Press, 2016, vol. 1.
- [12] M. Bilal, H. Kim, M. Fayaz, and P. Pawar, “Comparative analysis of time series forecasting approaches for household electricity consumption prediction,” 2022.
- [13] M. Hoffmann, L. Kotzur, D. Stolten, and M. Robinius, “A review on time series aggregation methods for energy system models,” *Energies*, vol. 13, no. 3, p. 641, 2020. [Online]. Available: <https://doi.org/10.3390/en13030641>
- [14] C. Duchon and R. Hale, “Time series analysis in meteorology and climatology: An introduction,” 2012.
- [15] J. Pearl, “Causal inference in statistics: An overview,” 2009.
- [16] E. N. Lorenz, *Empirical orthogonal functions and statistical weather prediction*. Massachusetts Institute of Technology, Department of Meteorology Cambridge, 1956, vol. 1.
- [17] ———, *Empirical orthogonal functions and statistical weather prediction*. Massachusetts Institute of Technology, Department of Meteorology Cambridge, 1956, vol. 1.
- [18] L. Li, X. Su, Y. Zhang, Y. Lin, and Z. Li, “Trend modeling for traffic time series analysis: An integrated study,” *IEEE Transactions on Intelligent Transportation Systems*, vol. 16, no. 6, pp. 3430–3439, 2015.
- [19] F. Al-Turjman, M. Nawaz, U. Ulusar, and R. I. Saeed, “Artificial intelligence-based traffic flow prediction: a comprehensive review,” *Journal of Electrical Systems and Information Technology*, 2023. [Online]. Available: <https://doi.org/10.1186/s43067-023-00081-6>
- [20] A. A. Ariyo, A. O. Adewumi, and C. K. Ayo, “Stock price prediction using the arima model,” 2014, pp. 106–112.
- [21] J. Hidalgo, “Journal of time series econometrics,” 2009. [Online]. Available: <https://www.degruyter.com/journal/key/jtse/html>
- [22] J. Lonlac, A. Doniec, M. Lujak, and S. Lecoeuche, “Extracting seasonal gradual patterns from temporal sequence data using periodic patterns mining,” 2020. [Online]. Available: <https://arxiv.org/abs/2010.10289>
- [23] C. Yang, X. Chen, L. Sun, and H. Yang, “Enhancing representation learning for periodic time series with floss: A frequency domain regularization approach,” 2023. [Online]. Available: <https://arxiv.org/pdf/2308.01011.pdf>
- [24] R. N. Bracewell, *The Fourier Transform and its Applications*. McGraw Hill, 1986.
- [25] R. Bracewell, “The fourier transform and its applications,” 2000. [Online]. Available: <https://books.google.com.ph/books?id=ecH2KgAACAAJ>
- [26] A. Vaswani, N. Shazeer, N. Parmar, J. Uszkoreit, L. Jones, A. N. Gomez, Ł. Kaiser, and I. Polosukhin, “Attention is all you need,” 2017.
- [27] Y. Liu, T. Hu, H. Zhang, H. Wu, S. Wang, L. Ma, and M. Long, “itransformer: Inverted transformers are effective for time series forecasting,” 2024. [Online]. Available: <https://arxiv.org/abs/2310.06625>
- [28] S. Bai, J. Z. Kolter, and V. Koltun, “An empirical evaluation of generic convolutional and recurrent networks for sequence modeling,” 2018.
- [29] H. Hewamalage, C. Bergmeir, and K. Bandara, “Recurrent neural networks for time series forecasting: Current status and future directions,” *International Journal of Forecasting*, vol. 37, no. 1, p. 388–427, Jan. 2021. [Online]. Available: <http://dx.doi.org/10.1016/j.ijforecast.2020.06.008>
- [30] Q. Wen, T. Zhou, C. Zhang, W. Chen, Z. Ma, J. Yan, and L. Sun, “Transformers in time series: A survey,” 2023.
- [31] K. Yi, Q. Zhang, L. Cao, S. Wang, G. Long, L. Hu, H. He, Z. Niu, W. Fan, and H. Xiong, “A survey on deep learning based time series analysis with frequency transformation,” 2023.

- [32] G. Chiarot and C. Silvestri, “Time series compression survey,” *ACM Computing Surveys*, vol. 55, no. 10, p. 1–32, Feb. 2023. [Online]. Available: <http://dx.doi.org/10.1145/3560814>
- [33] K. Yi, Q. Zhang, W. Fan, H. He, L. Hu, P. Wang, N. An, L. Cao, and Z. Niu, “Fouriergnn: Rethinking multivariate time series forecasting from a pure graph perspective,” 2023.
- [34] C. Zhu, X. Ma, W. Ding, and J. Zhan, “Long-term time series forecasting with multilinear trend fuzzy information granules for lstm in a periodic framework,” *IEEE Transactions on Fuzzy Systems*, vol. 32, no. 1, pp. 322–336, 2024.
- [35] Y. Hu and F. Xiao, “Time-series forecasting based on fuzzy cognitive visibility graph and weighted multisubgraph similarity,” *IEEE Transactions on Fuzzy Systems*, vol. 31, no. 4, pp. 1281–1293, 2022.
- [36] Y. Cheng, W. Xing, W. Pedrycz, S. Xian, and W. Liu, “Nfig-x: Non-linear fuzzy information granule series for long-term traffic flow time series forecasting,” 2023.
- [37] F. Li, Y. Tang, F. Yu, W. Pedrycz, Y. Liu, and W. Zeng, “Multilinear-trend fuzzy information granule-based short-term forecasting for time series,” *IEEE Transactions on Fuzzy Systems*, vol. 30, no. 8, pp. 3360–3372, 2021.
- [38] T. Zhan, Y. He, Y. Deng, and Z. Li, “Differential convolutional fuzzy time series forecasting,” 2023.
- [39] Y. Tang, F. Yu, W. Pedrycz, X. Yang, J. Wang, and S. Liu, “Building trend fuzzy granulation-based lstm recurrent neural network for long-term time-series forecasting,” *IEEE transactions on fuzzy systems*, vol. 30, no. 6, pp. 1599–1613, 2021.
- [40] K. Yi, Q. Zhang, W. Fan, S. Wang, P. Wang, H. He, D. Lian, N. An, L. Cao, and Z. Niu, “Frequency-domain mlps are more effective learners in time series forecasting,” 2023.
- [41] Z.-Q. J. Xu, “Frequency principle: Fourier analysis sheds light on deep neural networks,” *Communications in Computational Physics*, vol. 28, no. 5, p. 1746–1767, Jun. 2020. [Online]. Available: <http://dx.doi.org/10.4208/cicp.OA-2020-0085>
- [42] H. Wu, T. Hu, Y. Liu, H. Zhou, J. Wang, and M. Long, “Timesnet: Temporal 2d-variation modeling for general time series analysis,” 2023.
- [43] G. Woo, C. Liu, D. Sahoo, A. Kumar, and S. Hoi, “Cost: Contrastive learning of disentangled seasonal-trend representations for time series forecasting,” 2022.
- [44] Y. Nie, N. H. Nguyen, P. Sinthong, and J. Kalagnanam, “A time series is worth 64 words: Long-term forecasting with transformers,” 2023.
- [45] Y. Zhang and J. Yan, “Crossformer: Transformer utilizing cross-dimension dependency for multivariate time series forecasting,” 2023.
- [46] H. Wu, J. Xu, J. Wang, and M. Long, “Autoformer: Decomposition transformers with Auto-Correlation for long-term series forecasting,” 2021.
- [47] J. Li, X. Hui, and W. Zhang, “Informer: Beyond efficient transformer for long sequence time-series forecasting,” 2021.
- [48] Y. Liu, H. Wu, J. Wang, and M. Long, “Non-stationary transformers: Rethinking the stationarity in time series forecasting,” 2022.
- [49] T. Zhou, Z. Ma, Q. Wen, X. Wang, L. Sun, and R. Jin, “FEDformer: Frequency enhanced decomposed transformer for long-term series forecasting,” Baltimore, Maryland, 2022.
- [50] A. Zeng, M. Chen, L. Zhang, and Q. Xu, “Are transformers effective for time series forecasting?” 2023.
- [51] M. Liu, A. Zeng, M. Chen, Z. Xu, Q. Lai, L. Ma, and Q. Xu, “Scinet: time series modeling and forecasting with sample convolution and interaction,” 2022.
- [52] T. Zhou, Z. Ma, Q. Wen, L. Sun, T. Yao, W. Yin, R. Jin *et al.*, “Film: Frequency improved legendre memory model for long-term time series forecasting,” pp. 12 677–12 690, 2022.
- [53] K. Zhou, H. Yu, W. X. Zhao, and J.-R. Wen, “Filter-enhanced mlp is all you need for sequential recommendation,” ser. WWW ’22. ACM, Apr. 2022. [Online]. Available: <http://dx.doi.org/10.1145/3485447.3512111>
- [54] X. Zhang, Z. Zhao, T. Tsiligkaridis, and M. Zitnik, “Self-supervised contrastive pre-training for time series via time-frequency consistency,” 2022.
- [55] K. Xu, M. Qin, F. Sun, Y. Wang, Y.-K. Chen, and F. Ren, “Learning in the frequency domain,” 2020.
- [56] Z. Qin, P. Zhang, F. Wu, and X. Li, “Fcanet: Frequency channel attention networks,” 2021.

- [57] A. Paszke, S. Gross, F. Massa, A. Lerer, J. Bradbury, G. Chanan, T. Killeen, Z. Lin, N. Gimelshein, L. Antiga, A. Desmaison, A. Kopf, E. Yang, Z. DeVito, M. Raison, A. Tejani, S. Chilamkurthy, B. Steiner, L. Fang, J. Bai, and S. Chintala, “Pytorch: An imperative style, high-performance deep learning library,” *NeurIPS*, 2019.
- [58] D. P. Kingma and J. Ba, “Adam: A method for stochastic optimization,” *ICLR*, 2015.
- [59] A. Das, W. Kong, A. Leach, R. Sen, and R. Yu, “Long-term forecasting with tide: Time-series dense encoder,” 2023.
- [60] I. O. Tolstikhin, N. Houlsby, A. Kolesnikov, L. Beyer, X. Zhai, T. Unterthiner, J. Yung, A. Steiner, D. Keysers, J. Uszkoreit *et al.*, “Mlp-mixer: An all-mlp architecture for vision,” *NeurIPS*, 2021.
- [61] Y. Liu, C. Li, J. Wang, and M. Long, “Koopa: Learning non-stationary time series dynamics with koopman predictors,” 2023.
- [62] Bartlett, Peter, L. Mendelson, and Shahar, “Rademacher and gaussian complexities: Risk bounds and structural results.” *Journal of Machine Learning Research*, vol. 3, no. 3, pp. 463–463, 2003.
- [63] A. V. Oppenheim, R. W. Schafer, and J. R. Buck, “Discrete-time signal processing,” 1999.
- [64] D. R. Brillinger, *Time Series: Data Analysis and Theory*. Holden-Day, 1981.
- [65] H. So, “Discrete-time fourier transform,” *City University of Hong Kong*, 2024. [Online]. Available: [^1^][5]
- [66] G. E. P. Box, “Time Series Analysis.”
- [67] M. D. Adams, “Signals and Systems.”
- [68] J. D. Hamilton, “Time series analysis,” 2020.
- [69] D. G. Luenberger, “Dynamic systems,” 1979.
- [70] Y. LeCun, Y. Bengio, and G. Hinton, “Deep learning,” *Nature*, vol. 521, no. 7553, pp. 436–444, May 2015, number: 7553 Publisher: Nature Publishing Group. [Online]. Available: <https://www.nature.com/articles/nature14539>
- [71] L. C. Evans, *Partial differential equations*. American Mathematical Society, 2022, vol. 19. [Online]. Available: <https://books.google.com/books?hl=zh-CN&lr=&id=Ott1EAAAQBAJ&oi=fnd&pg=PP1&dq=Partial+Differential+Equations+evans&ots=cUNzAH2MyK&sig=yAAqmzvrLLXVgW7JzKTZ3qzvlqo>
- [72] A. V. Oppenheim, A. S. Willsky, S. H. Nawab, and J.-J. Ding, “Signals and systems,” 1997.
- [73] Y. Katznelson, “An introduction to harmonic analysis,” 2004.
- [74] G. E. Box, G. M. Jenkins, G. C. Reinsel, and G. M. Ljung, “Time series analysis: forecasting and control,” 2015.
- [75] H. J. Nussbaumer and H. J. Nussbaumer, “The fast fourier transform,” 1982.
- [76] Z. Yang, W. Yan, X. Huang, and L. Mei, “Adaptive temporal-frequency network for time-series forecasting,” *IEEE Transactions on Knowledge and Data Engineering*, vol. 34, no. 4, pp. 1576–1587, 2020.
- [77] P. C. Young, D. J. Pedregal, and W. Tych, “Dynamic harmonic regression,” *Journal of forecasting*, vol. 18, no. 6, pp. 369–394, 1999.
- [78] Z. Li, N. Kovachki, K. Azizzadenesheli, B. Liu, K. Bhattacharya, A. Stuart, and A. Anandkumar, “Fourier Neural Operator for Parametric Partial Differential Equations,” May 2021, arXiv:2010.08895 [cs, math]. [Online]. Available: <http://arxiv.org/abs/2010.08895>
- [79] H. Lange, S. L. Brunton, and J. N. Kutz, “From Fourier to Koopman: Spectral methods for long-term time series prediction,” *The Journal of Machine Learning Research*, vol. 22, no. 1, pp. 1881–1918, 2021, publisher: JMLRORG.
- [80] P. R. Winters, “Forecasting sales by exponentially weighted moving averages,” *Management science*, vol. 6, no. 3, pp. 324–342, 1960.
- [81] J. Mitrovic, B. McWilliams, J. Walker, L. Buesing, and C. Blundell, “Representation learning via invariant causal mechanisms,” *arXiv preprint arXiv:2010.07922*, 2020.
- [82] D. Liang, H. Zhang, D. Yuan, X. Ma, D. Li, and M. Zhang, “Does long-term series forecasting need complex attention and extra long inputs?” 2023.
- [83] Y. Zhao, Z. Ma, T. Zhou, M. Ye, L. Sun, and Y. Qian, “Gcformer: An efficient solution for accurate and scalable long-term multivariate time series forecasting,” ser. CIKM ’23. New York, NY, USA: Association for Computing Machinery, 2023, p. 3464–3473. [Online]. Available: <https://doi.org/10.1145/3583780.3615136>
- [84] D. Du, B. Su, and Z. Wei, “Preformer: Predictive transformer with multi-scale segment-wise correlations for long-term time series forecasting,” IEEE, 2023.

- [85] P. Tang and X. Zhang, “Infomaxformer: Maximum entropy transformer for long time-series forecasting problem,” 2023.
- [86] J. Guo, Z. Wan, and Z. Lv, “Digital twins fuzzy system based on time series forecasting model lftformer,” ser. MM ’23. New York, NY, USA: Association for Computing Machinery, 2023, p. 7094–7100. [Online]. Available: <https://doi.org/10.1145/3581783.3612936>
- [87] Z. Xu, A. Zeng, and Q. Xu, “FITS: Modeling time series with \$10k\$ parameters,” 2024. [Online]. Available: <https://openreview.net/forum?id=bWcnvZ3qMb>
- [88] P. Chen, Y. ZHANG, Y. Cheng, Y. Shu, Y. Wang, Q. Wen, B. Yang, and C. Guo, “Pathformer: Multi-scale transformers with adaptive pathways for time series forecasting,” 2024.
- [89] S. Wang, H. Wu, X. Shi, T. Hu, H. Luo, L. Ma, J. Y. Zhang, and J. ZHOU, “Timemixer: Decomposable multiscale mixing for time series forecasting,” 2024. [Online]. Available: <https://openreview.net/forum?id=7oLshfEIC2>
- [90] H. Kim, S. Kim, S. Min, and B. Lee, “Contrastive time-series anomaly detection,” no. 01, pp. 1–14, nov 5555.
- [91] J. Zhang, W. Li, W. Sun, Y. Zhang, and R. Tao, “Locality robust domain adaptation for cross-scene hyperspectral image classification,” MAR 15 2024.
- [92] J. Zhang, J. Wang, W. Qiang, F. Xu, C. Zheng, F. Sun, and H. Xiong, “Intriguing properties of positional encoding in time series forecasting,” 2024.
- [93] J. Wang, Y. Zhou, W. Qiang, Y. Ba, B. Su, and J.-R. Wen, “Spatio-temporal branching for motion prediction using motion increments,” pp. 4290–4299, 2023.
- [94] X. Zhang, S. Zhao, Z. Song, H. Guo, J. Zhang, C. Zheng, and W. Qiang, “Not all frequencies are created equal:towards a dynamic fusion of frequencies in time-series forecasting,” 2024. [Online]. Available: <https://arxiv.org/abs/2407.12415>
- [95] Z. Li, S. Qi, Y. Li, and Z. Xu, “Revisiting long-term time series forecasting: An investigation on linear mapping,” *ArXiv*, vol. abs/2305.10721, 2023.
- [96] G. W. Imbens and D. B. Rubin, *Causal Inference for Statistics, Social, and Biomedical Sciences: An Introduction*. Cambridge University Press, 2015.
- [97] J. Li, B. Wu, X. Sun, and Y. Wang, “Causal hidden markov model for time series disease forecasting,” 2021, pp. 12 100–12 109.
- [98] Y. Wang, H. Wu, J. Dong, G. Qin, H. Zhang, Y. Liu, Y. Qiu, J. Wang, and M. Long, “Timexer: Empowering transformers for time series forecasting with exogenous variables,” 2024. [Online]. Available: <https://arxiv.org/abs/2402.19072>
- [99] Y. Liu, G. Qin, X. Huang, J. Wang, and M. Long, “Timer-XL: Long-context transformers for unified time series forecasting,” 2025. [Online]. Available: <https://openreview.net/forum?id=KMCJXjlDDr>
- [100] Y. Yamaguchi, I. Suemitsu, and W. Wei, “Citras: Covariate-informed transformer for time series forecasting,” 2025. [Online]. Available: <https://arxiv.org/abs/2503.24007>
- [101] M. Liu, X. Sun, L. Hu, and Y. Wang, “Causal discovery from subsampled time series with proxy variables,” 2023. [Online]. Available: <https://openreview.net/forum?id=etYk6TeO2q>
- [102] A. A. Mastakouri, B. Schölkopf, and D. Janzing, “Necessary and sufficient conditions for causal feature selection in time series with latent common causes,” ser. Proceedings of Machine Learning Research, M. Meila and T. Zhang, Eds., vol. 139. PMLR, 18–24 Jul 2021, pp. 7502–7511. [Online]. Available: <https://proceedings.mlr.press/v139/mastakouri21a.html>
- [103] M. Castro, P. Júnior, A. Soriano Vargas, R. Werneck, M. Gonçalves, L. Lusquino Filho, R. Moura, M. Zampieri, O. Linares, V. Ferreira, A. Ferreira, A. Davolio, D. Schiozer, and A. Rocha, “Time series causal relationships discovery through feature importance and ensemble models,” *Scientific Reports*, vol. 13, 07 2023.
- [104] D. S. Wilks, *Statistical methods in the atmospheric sciences*. Academic press, 2011.
- [105] M. Glymour, J. Pearl, and N. P. Jewell, *Causal Inference in Statistics: A Primer*. John Wiley & Sons, Jan. 2016.
- [106] J. Pearl, *Causality*. Cambridge university press, 2009.
- [107] M. Mohri, A. Rostamizadeh, and A. Talwalkar, *Foundations of Machine Learning*. MIT press, 2018.
- [108] V. Kuznetsov and M. Mohri, “Generalization Bounds for Time Series Prediction with Non-stationary Processes,” P. Auer, A. Clark, T. Zeugmann, and S. Zilles, Eds. Cham: Springer International Publishing, 2014, vol. 8776, pp. 260–274.

- [109] C. W. Granger, “Investigating causal relations by econometric models and cross-spectral methods,” *Econometrica: journal of the Econometric Society*, pp. 424–438, 1969.
- [110] A. P. Dawid, “Conditional independence in statistical theory,” *Journal of the Royal Statistical Society Series B: Statistical Methodology*, vol. 41, no. 1, pp. 1–15, 1979.
- [111] J. Pearl, “Embracing causality in default reasoning,” *Artificial Intelligence*, vol. 35, no. 2, pp. 259–271, 1988.
- [112] J. Pearl and A. Paz, “Graphoids: Graph-based logic for reasoning about relevance relations or when would x tell you more about y if you already know z ?” 2022, pp. 189–200.
- [113] A. Statnikov, N. I. Lytkin, J. Lemeire, and C. F. Aliferis, “Algorithms for discovery of multiple markov boundaries,” *Journal of Machine Learning Research*, vol. 14, no. Feb, pp. 499–566, 2013.
- [114] E. S. Gardner Jr, “Exponential smoothing: The state of the art,” *Journal of forecasting*, vol. 4, no. 1, pp. 1–28, 1985.
- [115] B. Lim and S. Zohren, “Time-series forecasting with deep learning: a survey,” *Philosophical Transactions of the Royal Society A*, vol. 379, no. 2194, p. 20200209, 2021.
- [116] A. C. Harvey, “Forecasting, structural time series models and the kalman filter,” 1990.
- [117] L. G. Valiant, “A theory of the learnable,” *Communications of the ACM*, vol. 27, no. 11, pp. 1134–1142, 1984.
- [118] V. Koltchinskii, “Rademacher penalties and structural risk minimization,” *IEEE Transactions on Information Theory*, vol. 47, no. 5, pp. 1902–1914, 2001.
- [119] V. N. Vapnik and A. Y. Chervonenkis, “On uniform convergence of the frequencies of events to their probabilities,” *Teoriya Veroyatnostei i ee Primeneniya*, vol. 16, no. 2, pp. 264–279, 1971.
- [120] P. Doukhan and P. Doukhan, “Mixing,” *Mixing: Properties and Examples*, pp. 15–23, 1994.
- [121] B. Yu, “Rates of convergence for empirical processes of stationary mixing sequences,” *The Annals of Probability*, pp. 94–116, 1994.
- [122] A. Rakhlin, K. Sridharan, and A. Tewari, “Online learning: Random averages, combinatorial parameters, and learnability,” *Advances in Neural Information Processing Systems*, vol. 23, 2010.
- [123] V. Kuznetsov and M. Mohri, “Learning Theory and Algorithms for Forecasting Non-stationary Time Series,” vol. 28. Curran Associates, Inc., 2015.
- [124] A. R. Statnikov, J. Lemeir, and C. F. Aliferis, “Algorithms for discovery of multiple markov boundaries,” *Journal of Machine Learning Research Jmlr*, 2013.
- [125] S. L. Lauritzen and N. Wermuth, “Graphical models for associations between variables, some of which are qualitative and some quantitative,” *The annals of Statistics*, pp. 31–57, 1989.
- [126] B. Sibbald and M. Roland, “Understanding controlled trials. why are randomised controlled trials important?” *BMJ: British Medical Journal*, vol. 316, no. 7126, p. 201, 1998.
- [127] P. Spirtes and C. Glymour, “An algorithm for fast recovery of sparse causal graphs,” *Social science computer review*, vol. 9, no. 1, pp. 62–72, 1991.
- [128] T. Verma and J. Pearl, “Causal networks: Semantics and expressiveness.” Elsevier, 1990, vol. 9, pp. 69–76.
- [129] P. Spirtes, C. Glymour, and R. Scheines, *Causation, prediction, and search*. MIT press, 2001.
- [130] R. Cai, K. Zhang, R. Guo, and et al., “Causallearn: Causal discovery library,” *arXiv preprint arXiv:2301.01703*, 2023.
- [131] P. Spirtes, “An anytime algorithm for causal inference.” PMLR, 2001, pp. 278–285.
- [132] D. Entner and P. O. Hoyer, “On causal discovery from time series data using fci,” *Probabilistic graphical models*, vol. 16, 2010.
- [133] D. Koller and N. Friedman, *Probabilistic Graphical Models: Principles and Techniques*. Probabilistic Graphical Models: Principles and Techniques, 2009.
- [134] D. Wang, R. Liu, C. Chen, and S. Li, “Mpm: Multi patterns memory model for short-term time series forecasting,” *IEEE Trans. on Knowl. and Data Eng.*, vol. 37, no. 1, p. 438–448, Jan. 2025. [Online]. Available: <https://doi.org/10.1109/TKDE.2024.3490843>
- [135] K. Yan, C. Long, H. Wu, and Z. Wen, “Multi-resolution expansion of analysis in time-frequency domain for time series forecasting,” *IEEE Trans. on Knowl. and Data Eng.*, vol. 36, no. 11, p. 6667–6680, Nov. 2024. [Online]. Available: <https://doi.org/10.1109/TKDE.2024.3396785>

- [136] S. Feng, C. Miao, K. Xu, J. Wu, P. Wu, Y. Zhang, and P. Zhao, “Multi-scale attention flow for probabilistic time series forecasting,” *IEEE Trans. on Knowl. and Data Eng.*, vol. 36, no. 5, p. 2056–2068, May 2024. [Online]. Available: <https://doi.org/10.1109/TKDE.2023.3319672>
- [137] M. Jin, Y. Zheng, Y.-F. Li, S. Chen, B. Yang, and S. Pan, “Multivariate time series forecasting with dynamic graph neural odes,” *IEEE Trans. on Knowl. and Data Eng.*, vol. 35, no. 9, p. 9168–9180, Sep. 2023. [Online]. Available: <https://doi.org/10.1109/TKDE.2022.3221989>
- [138] L. Chen, D. Chen, Z. Shang, B. Wu, C. Zheng, B. Wen, and W. Zhang, “Multi-scale adaptive graph neural network for multivariate time series forecasting,” *IEEE Trans. on Knowl. and Data Eng.*, vol. 35, no. 10, p. 10748–10761, Oct. 2023. [Online]. Available: <https://doi.org/10.1109/TKDE.2023.3268199>
- [139] L. Li, J. Yan, Y. Zhang, J. Zhang, J. Bao, Y. Jin, and X. Yang, “Learning generative rnn-ode for collaborative time-series and event sequence forecasting,” *IEEE Trans. on Knowl. and Data Eng.*, vol. 35, no. 7, p. 7118–7137, Jul. 2023. [Online]. Available: <https://doi.org/10.1109/TKDE.2022.3185115>
- [140] C. Gong, D. Yao, C. Zhang, W. Li, J. Bi, L. Du, and J. Wang, “Causal discovery from temporal data,” ser. KDD ’23. New York, NY, USA: Association for Computing Machinery, 2023. [Online]. Available: <https://doi.org/10.1145/3580305.3599552>
- [141] F. Takens, “Detecting strange attractors in turbulence.” Springer, 1981, pp. 366–381.
- [142] H. Xue and F. D. Salim, “Promptcast: A new prompt-based learning paradigm for time series forecasting,” 2023. [Online]. Available: <https://arxiv.org/abs/2210.08964>
- [143] N. Gruver, M. Finzi, S. Qiu, and A. G. Wilson, “Large language models are zero-shot time series forecasters,” 2024. [Online]. Available: <https://arxiv.org/abs/2310.07820>
- [144] T. Zhou, P. Niu, X. Wang, L. Sun, and R. Jin, “One fits all: power general time series analysis by pretrained lm,” 2023. [Online]. Available: <https://arxiv.org/abs/2302.11939>
- [145] X. Liu, J. Hu, Y. Li, S. Diao, Y. Liang, B. Hooi, and R. Zimmermann, “Unitime: A language-empowered unified model for cross-domain time series forecasting,” 2024. [Online]. Available: <https://arxiv.org/abs/2310.09751>
- [146] M. Jin, S. Wang, L. Ma, Z. Chu, J. Y. Zhang, X. Shi, P.-Y. Chen, Y. Liang, Y.-F. Li, S. Pan, and Q. Wen, “Time-llm: Time series forecasting by reprogramming large language models,” 2024. [Online]. Available: <https://arxiv.org/abs/2310.01728>
- [147] D. Cao, F. Jia, S. O. Arik, T. Pfister, Y. Zheng, W. Ye, and Y. Liu, “Tempo: Prompt-based generative pre-trained transformer for time series forecasting,” 2024. [Online]. Available: <https://arxiv.org/abs/2310.04948>
- [148] Z. Tong, H. Li, and Y. Zhang, “A comparison of arima, lstm, xgboost and hybrid in stock price prediction,” in *2023 5th International Conference on Applied Machine Learning (ICAML)*, 2023, pp. 18–25.
- [149] Y. Liu, G. Qin, X. Huang, J. Wang, and M. Long, “Autotimes: autoregressive time series forecasters via large language models,” in *Proceedings of the 38th International Conference on Neural Information Processing Systems*, ser. NIPS ’24. Red Hook, NY, USA: Curran Associates Inc., 2025.
- [150] H. Touvron, L. Martin, K. Stone, P. Albert, A. Almahairi, Y. Babaei, N. Bashlykov, S. Batra, P. Bhargava, S. Bhosale, D. Bikel, L. Blecher, C. C. Ferrer, M. Chen, G. Cucurull, D. Esiobu, J. Fernandes, J. Fu, W. Fu, B. Fuller, C. Gao, V. Goswami, N. Goyal, A. Hartshorn, S. Hosseini, R. Hou, H. Inan, M. Kardas, V. Kerkez, M. Khabsa, I. Kloumann, A. Korenev, P. S. Koura, M.-A. Lachaux, T. Lavril, J. Lee, D. Liskovich, Y. Lu, Y. Mao, X. Martinet, T. Mihaylov, P. Mishra, I. Molybog, Y. Nie, A. Poulton, J. Reizenstein, R. Rungta, K. Saladi, A. Schelten, R. Silva, E. M. Smith, R. Subramanian, X. E. Tan, B. Tang, R. Taylor, A. Williams, J. X. Kuan, P. Xu, Z. Yan, I. Zarov, Y. Zhang, A. Fan, M. Kambadur, S. Narang, A. Rodriguez, R. Stojnic, S. Edunov, and T. Scialom, “Llama 2: Open foundation and fine-tuned chat models,” 2023. [Online]. Available: <https://arxiv.org/abs/2307.09288>
- [151] T. B. Brown, B. Mann, N. Ryder, M. Subbiah, J. Kaplan, P. Dhariwal, A. Neelakantan, P. Shyam, G. Sastry, A. Askell, S. Agarwal, A. Herbert-Voss, G. Krueger, T. Henighan, R. Child, A. Ramesh, D. M. Ziegler, J. Wu, C. Winter, C. Hesse, M. Chen, E. Sigler, M. Litwin, S. Gray, B. Chess, J. Clark, C. Berner, S. McCandlish, A. Radford, I. Sutskever, and D. Amodei, “Language models are few-shot learners,” 2020. [Online]. Available: <https://arxiv.org/abs/2005.14165>
- [152] S. Zhang, S. Roller, N. Goyal, M. Artetxe, M. Chen, S. Chen, C. Dewan, M. Diab, X. Li, X. V. Lin, T. Mihaylov, M. Ott, S. Shleifer, K. Shuster, D. Simig, P. S. Koura, A. Sridhar, T. Wang, and L. Zettlemoyer, “Opt: Open pre-trained transformer language models,” 2022. [Online]. Available: <https://arxiv.org/abs/2205.01068>
- [153] T. B. Brown, B. Mann, N. Ryder, M. Subbiah, J. Kaplan, P. Dhariwal, A. Neelakantan, P. Shyam, G. Sastry, A. Askell, S. Agarwal, A. Herbert-Voss, G. Krueger, T. Henighan, R. Child, A. Ramesh, D. M. Ziegler, J. Wu,

C. Winter, C. Hesse, M. Chen, E. Sigler, M. Litwin, S. Gray, B. Chess, J. Clark, C. Berner, S. McCandlish, A. Radford, I. Sutskever, and D. Amodei, “Language models are few-shot learners,” 2020. [Online]. Available: <https://arxiv.org/abs/2005.14165>

[154] Y. Hu, Q. Li, D. Zhang, J. Yan, and Y. Chen, “Context-alignment: Activating and enhancing LLMs capabilities in time series,” in *The Thirteenth International Conference on Learning Representations*, 2025. [Online]. Available: <https://openreview.net/forum?id=syC2764fPc>

[155] M. Tan, M. A. Merrill, V. Gupta, T. Althoff, and T. Hartvigsen, “Are language models actually useful for time series forecasting?” in *The Thirty-eighth Annual Conference on Neural Information Processing Systems*, 2024. [Online]. Available: <https://openreview.net/forum?id=DV15UbHCY1>

[156] T. Wang, A. Roberts, D. Hesslow, T. L. Scao, H. W. Chung, I. Beltagy, J. Launay, and C. Raffel, “What language model architecture and pretraining objective work best for zero-shot generalization?” 2022. [Online]. Available: <https://arxiv.org/abs/2204.05832>

[157] D. Dai, Y. Sun, L. Dong, Y. Hao, S. Ma, Z. Sui, and F. Wei, “Why can gpt learn in-context? language models implicitly perform gradient descent as meta-optimizers,” 2023. [Online]. Available: <https://arxiv.org/abs/2212.10559>

[158] M. Ranzato, S. Chopra, M. Auli, and W. Zaremba, “Sequence level training with recurrent neural networks,” in *4th International Conference on Learning Representations, ICLR 2016, San Juan, Puerto Rico, May 2-4, 2016, Conference Track Proceedings*, Y. Bengio and Y. LeCun, Eds., 2016. [Online]. Available: <http://arxiv.org/abs/1511.06732>

[159] H. Lee and S. Chen, “A systematic bias of machine learning regression models and its correction: an application to imaging-based brain age prediction,” 2024. [Online]. Available: <https://arxiv.org/abs/2405.15950>

[160] V. A. Satopää, M. Salikhov, P. E. Tetlock, and B. Mellers, “Bias, information, noise: The bin model of forecasting,” *Manage. Sci.*, vol. 67, no. 12, p. 7599–7618, Dec. 2021. [Online]. Available: <https://doi.org/10.1287/mnsc.2020.3882>

[161] A. Goyal, A. Lamb, Y. Zhang, S. Zhang, A. Courville, and Y. Bengio, “Professor forcing: a new algorithm for training recurrent networks,” in *Proceedings of the 30th International Conference on Neural Information Processing Systems*, ser. NIPS’16. Red Hook, NY, USA: Curran Associates Inc., 2016, p. 4608–4616.

[162] A. Namazi, A. D. Fathkouhi, and H. Shakeri, “Mitigating exposure bias in risk-aware time series forecasting with soft tokens,” 2025. [Online]. Available: <https://arxiv.org/abs/2512.10056>

[163] F. Schmidt, “Generalization in generation: A closer look at exposure bias,” in *Proceedings of the 3rd Workshop on Neural Generation and Translation*, A. Birch, A. Finch, H. Hayashi, I. Konstas, T. Luong, G. Neubig, Y. Oda, and K. Sudoh, Eds. Hong Kong: Association for Computational Linguistics, Nov. 2019, pp. 157–167. [Online]. Available: <https://aclanthology.org/D19-5616/>

[164] S. Ross, G. J. Gordon, and J. A. Bagnell, “A reduction of imitation learning and structured prediction to no-regret online learning,” 2011. [Online]. Available: <https://arxiv.org/abs/1011.0686>

[165] X. Ma, Z.-L. Ni, S. Xiao, and X. Chen, “Timepro: Efficient multivariate long-term time series forecasting with variable- and time-aware hyper-state,” in *Forty-second International Conference on Machine Learning*, 2025. [Online]. Available: <https://openreview.net/forum?id=s69Ei2VrIW>

[166] Y. Sun, Z. Xie, E. Eldele, D. Chen, Q. Hu, and M. Wu, “Learning pattern-specific experts for time series forecasting under patch-level distribution shift,” in *The Thirty-ninth Annual Conference on Neural Information Processing Systems*, 2025. [Online]. Available: <https://openreview.net/forum?id=CtoIG9Iwas>

[167] J. Zhang, J. Wang, W. Qiang, F. Xu, and C. Zheng, “Enhancing large language models for time-series forecasting via vector-injected in-context learning,” *arXiv preprint arXiv:2601.07903*, 2026.

[168] H. Chen, V. Luong, L. Mukherjee, and V. Singh, “Simpletm: A simple baseline for multivariate time series forecasting,” in *The Thirteenth International Conference on Learning Representations*, 2025.

[169] S. Wang, J. Li, X. Shi, Z. Ye, B. Mo, W. Lin, J. Shengtong, Z. Chu, and M. Jin, “Timemixer++: A general time series pattern machine for universal predictive analysis,” in *ICLR 2025: The Thirteenth International Conference on Learning Representations*. International Conference on Learning Representations, 2025.

Appendix A provides the implementation details of F-LLM. Appendix B provides the description of the dataset. Appendix C provides the proof of Proposition 4.1. Appendix D provides the proof of Theorem 4.1. Appendix E provides full prediction results. Appendix F prevents the comparison of the results among F-LLM, Autotimes, and PatchTST.

A Implementation Details

All experiments are implemented in PyTorch [57] and trained on NVIDIA V100 32GB GPUs. The model is based on a frozen LLaMA-2-7B [150] backbone, with all LLM parameters kept fixed during training. A linear encoder and decoder are used to project time series patches to LLM hidden space (dimension 4096) and back time series space, while a lightweight linear bias predictor f_b models the residual correction. The Adam optimizer [58] is used with a learning rate selected from $\{10^{-3}, 10^{-4}\}$ and batch size from $\{128, 224\}$ based on performance. Training proceeds for up to 10 epochs using Mean Squared Error (MSE) loss, with early stopping applied when validation loss does not improve for three epochs. Inputs are standardized by channel-wise mean and variance before embedding, and outputs are rescaled back to their original magnitudes after decoding. Each experiment is repeated five times with different random seeds, and both MSE and Mean Absolute Error (MAE) are reported.

B Data Description

In this paper, we conduct tests using five real-world datasets. These datasets include: (1) ETT contains two sub-datasets: ETT1 and ETT2, collected from two electricity transformers at two stations. Each of them has two versions in different resolutions (15 minutes and 1h). ETT dataset contains multiple series of loads and one series of oil temperatures. (2) Weather covers 21 meteorological variables recorded at 10-minute intervals throughout the year 2020. The data was collected by the Max Planck Institute for Biogeochemistry’s Weather Station, providing valuable meteorological insights. (3) ECL records the hourly electricity consumption data of 321 clients. (4) Traffic gathers hourly road occupancy rates from 862 sensors on San Francisco Bay area freeways, covering the period from January 2015 to December 2016. (5) M4 is a competition dataset encompassing various time series across different frequencies and domains, such as business and economics. (6) M3, albeit smaller than M4, also contains diverse time series from various domains.

We follow the same data processing and train-validation-test set split protocol used in Autotimes [149], where the train, validation, and test datasets are strictly divided according to chronological order to ensure no data leakage. As for long-term forecasting settings, we fix the context length of F-LLM and the lookback length of other compared methods as 672 in ETT, ECL, Traffic, Weather, and Solar-Energy, and the forecast length varies in $\{96, 192, 336, 720\}$. For M3 and M4, the look-back length equals twice the forecast length. The details are provided in Table 7.

C Proof of Proposition 4.1

Proof C.1 *By recursively applying the linearized transition Eq. (3) for H steps, the accumulated error at step $t + H$ can be expressed as:*

$$\Delta x_{t+H} \approx J_g^H \Delta x_t + \sum_{k=0}^{H-1} J_g^{H-1-k} \epsilon_{t+k}. \quad (14)$$

Taking the norm and applying the triangle inequality yields:

$$\|\Delta x_{t+H}\| \leq \|J_g^H\| \|\Delta x_t\| + \sum_{k=0}^{H-1} \|J_g^{H-1-k}\| \|\epsilon_{t+k}\|. \quad (15)$$

According to Gelfand’s formula, for any matrix norm, $\lim_{k \rightarrow \infty} \|J_g^k\|^{1/k} = \rho(J_g)$. Thus, for a sufficiently large k , $\|J_g^k\|$ behaves asymptotically as $\rho(J_g)^k$. Assuming the single-step error is bounded by γ , the dominant term in the summation is a geometric series governed by $\rho(J_g)$. Consequently, if $\rho(J_g) > 1$, both the transient term (related to initial error) and the accumulated noise term scale according to $\mathcal{O}(\rho(J_g)^H)$, leading to divergence.

D Proof of Theorem 4.1

Proof D.1 *Consider the closed-loop error dynamics approximated by $\Delta x_t \approx (J_g - L)\Delta x_{t-1} + \epsilon_t$. Taking the Euclidean norm on both sides and applying the triangle inequality yields the recurrence relation $\|\Delta x_t\| \leq \|J_g - L\| \|\Delta x_{t-1}\| + \|\epsilon_t\|$.*

$L\|_2\|\Delta x_{t-1}\| + \|\epsilon_t\|$. Substituting the assumptions $\|J_g - L\|_2 \leq q$ and $\|\epsilon_t\| \leq \gamma$, we obtain $\|\Delta x_t\| \leq q\|\Delta x_{t-1}\| + \gamma$. By recursively unfolding this inequality from step t back to the initial step 0, we get:

$$\|\Delta x_t\| \leq q^t \|\Delta x_0\| + \gamma \sum_{k=0}^{t-1} q^k. \quad (16)$$

Since $q \in [0, 1)$, the first term $q^t \|\Delta x_0\|$ vanishes as $t \rightarrow \infty$. The second term is a geometric series which converges to $\gamma \frac{1-q^t}{1-q}$. Taking the limit superior as $t \rightarrow \infty$, the upper bound becomes $\frac{\gamma}{1-q}$. Thus, the error does not accumulate indefinitely but remains confined within a fixed radius.

Dataset	Dim	Prediction Length	Dataset Size	Frequency	Information
ETTh1,ETTh2	7	{96, 192, 336, 720}	(8545, 2881, 2881)	Hourly	Electricity
ETTm1,ETTm2	7	{96, 192, 336, 720}	(34465, 11521, 11521)	15min	Electricity
Weather	21	{96, 192, 336, 720}	(36792, 5271, 10540)	10min	Weather
ECL	321	{96, 192, 336, 720}	(18317, 2633, 5261)	Hourly	Electricity
Traffic	862	{96, 192, 336, 720}	(12185, 1757, 3509)	Hourly	Transportation
M4-Yearly	1	6	(23000, 0, 23000)	Yearly	Demographic
M4-Quarterly	1	8	(24000, 0, 24000)	Quarterly	Finance
M4-Monthly	1	18	(48000, 0, 48000)	Monthly	Industry
M4-Weekly	1	13	(359, 0, 359)	Weekly	Macro
M4-Daily	1	14	(4227, 0, 4227)	Daily	Micro
M4-Hourly	1	48	(414, 0, 414)	Hourly	Other
M3-Yearly	1	6	(645, 0, 645)	Yearly	Demographic
M3-Quarterly	1	8	(756, 0, 756)	Quarterly	Finance
M3-Monthly	1	18	(1428, 0, 1428)	Monthly	Industry
M3-Others	1	8	(174, 0, 174)	Weekly	Macro

Table 7: Detailed descriptions of datasets. *Dim* denotes the number of variables in each dataset. *Prediction Length* denotes the number of future time points to predict; each dataset includes four different forecasting horizons. *Time steps* represents the number of time points. *Percentage* indicates the proportions of the dataset allocated to Train, Validation, and Test splits. *Frequency* specifies the sampling interval between consecutive time points.

E Full Forecasting Results

The full multivariate forecasting results are provided in Table 8. All results are averaged over five random seeds.

F Compare prediction results

Figure 6-8 compares F-LLM (input window 672, prediction 96) with Autotimes and PatchTST on the ETTh1, ETTh2, and Weather datasets.

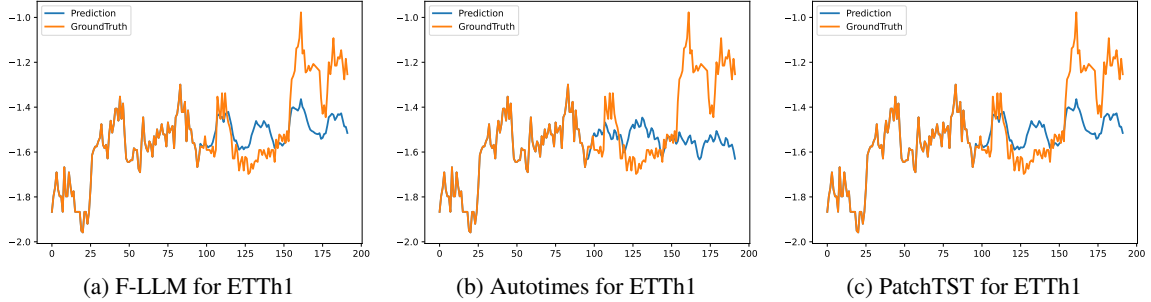


Figure 6: Visualization of forecasting results for the ETTh1 dataset under the input-672-predict-96 setting. Only display the last 96 input time points.

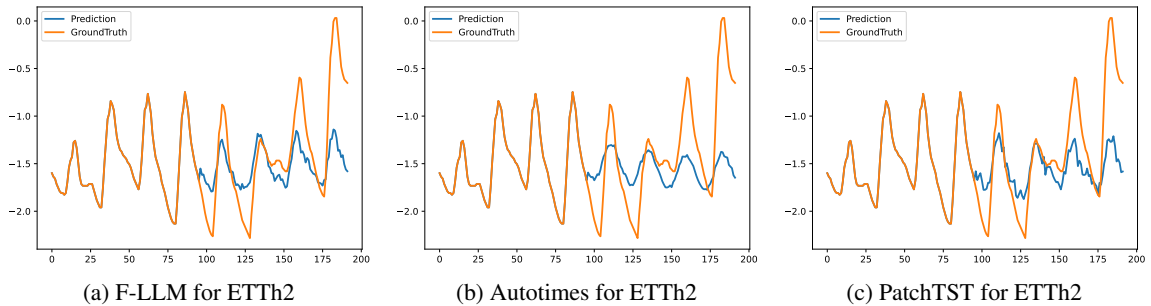


Figure 7: Visualization of forecasting results for the ETTh2 dataset under the input-672-predict-96 setting. Only display the last 96 input time points.

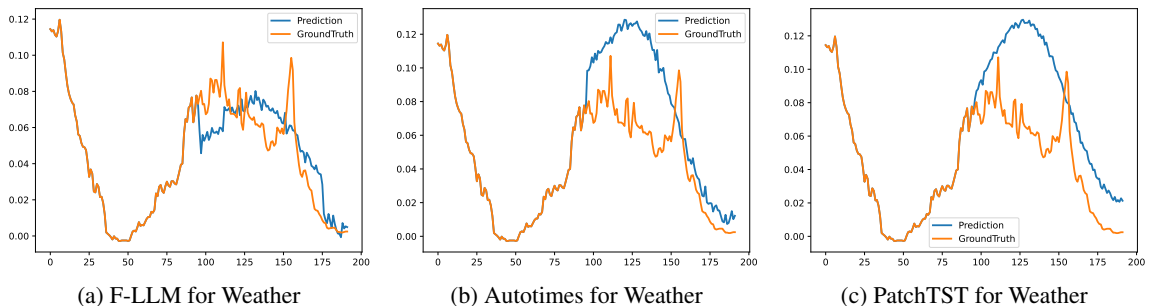


Figure 8: Visualization of forecasting results for the Weather dataset under the input-672-predict-96 setting. Only display the last 96 input time points.

Method	F-LLM	AutoTimes	LVICL	TimeLLM	FPT	Unitime	iTransformer	DLinear	PatchTST	TimesNet	TimeMixer++	SimpleTM	
	Ours (2024)	(2026)	(2024)	(2023)	(2024)	(2023)	(2023)	(2023)	(2023)	(2023)	(2025)	(2025)	
Metric	MSE	MAE	MSE	MAE	MSE	MAE	MSE	MAE	MSE	MAE	MSE	MAE	
ETTh1	96	0.347 0.379	0.360 0.400	0.351 0.389	0.362 0.392	0.376 0.397	0.397 0.418	0.386 0.405	0.375 0.399	0.370 0.399	0.384 0.402	0.355 0.391	0.350 0.375
	192	0.375 0.402	0.388 0.419	0.379 0.408	0.398 0.418	0.416 0.418	0.434 0.439	0.422 0.439	0.405 0.416	0.413 0.421	0.557 0.436	0.406 0.430	0.402 0.405
	336	0.390 0.415	0.401 0.429	0.392 0.417	0.430 0.427	0.442 0.433	0.468 0.458	0.444 0.457	0.439 0.443	0.422 0.436	0.491 0.469	0.423 0.427	0.416 0.419
	720	0.395 0.427	0.406 0.440	0.402 0.434	0.442 0.457	0.477 0.456	0.469 0.477	0.500 0.498	0.472 0.490	0.447 0.466	0.521 0.500	0.461 0.438	0.442 0.442
ETTh2	Avg	0.376 0.405	0.389 0.422	0.381 0.412	0.408 0.424	0.428 0.426	0.442 0.448	0.438 0.450	0.423 0.437	0.413 0.430	0.488 0.452	0.411 0.421	0.403 0.410
	96	0.261 0.324	0.288 0.342	0.270 0.332	0.288 0.341	0.287 0.341	0.297 0.354	0.304 0.360	0.289 0.353	0.274 0.336	0.340 0.374	0.269 0.322	0.271 0.323
	192	0.324 0.369	0.348 0.387	0.333 0.378	0.351 0.389	0.350 0.383	0.365 0.404	0.377 0.403	0.383 0.418	0.339 0.379	0.402 0.414	0.337 0.368	0.338 0.373
	336	0.315 0.371	0.365 0.412	0.325 0.377	0.362 0.401	0.373 0.395	0.359 0.401	0.405 0.429	0.448 0.465	0.329 0.380	0.452 0.452	0.341 0.392	0.345 0.385
ETTm1	720	0.368 0.405	0.412 0.440	0.375 0.416	0.415 0.440	0.401 0.443	0.403 0.436	0.443 0.464	0.605 0.551	0.379 0.422	0.462 0.468	0.383 0.404	0.399 0.413
	Avg	0.317 0.367	0.352 0.395	0.326 0.376	0.354 0.393	0.353 0.391	0.356 0.399	0.382 0.414	0.431 0.447	0.330 0.379	0.414 0.427	0.333 0.371	0.338 0.374
	96	0.262 0.329	0.274 0.343	0.269 0.343	0.284 0.341	0.301 0.343	0.308 0.358	0.312 0.366	0.299 0.343	0.290 0.342	0.338 0.375	0.303 0.324	0.311 0.340
	192	0.300 0.363	0.316 0.370	0.309 0.371	0.327 0.363	0.348 0.362	0.354 0.391	0.347 0.385	0.335 0.365	0.332 0.369	0.374 0.387	0.339 0.355	0.347 0.366
ETTm2	336	0.335 0.380	0.344 0.390	0.343 0.390	0.368 0.387	0.386 0.397	0.396 0.413	0.379 0.404	0.369 0.386	0.366 0.392	0.410 0.411	0.365 0.381	0.367 0.382
	720	0.379 0.399	0.392 0.418	0.391 0.408	0.423 0.419	0.410 0.427	0.442 0.450	0.441 0.442	0.425 0.421	0.416 0.420	0.478 0.450	0.433 0.415	0.428 0.424
	Avg	0.319 0.367	0.332 0.380	0.328 0.378	0.350 0.378	0.366 0.382	0.375 0.403	0.370 0.399	0.357 0.379	0.351 0.381	0.400 0.406	0.360 0.369	0.363 0.378
	96	0.151 0.240	0.159 0.250	0.155 0.246	0.168 0.250	0.172 0.258	0.179 0.265	0.179 0.271	0.167 0.269	0.165 0.255	0.187 0.267	0.168 0.239	0.164 0.247
ECL	192	0.206 0.278	0.213 0.285	0.210 0.282	0.216 0.294	0.231 0.287	0.239 0.309	0.242 0.313	0.224 0.303	0.220 0.292	0.249 0.309	0.223 0.283	0.226 0.290
	336	0.254 0.314	0.261 0.323	0.258 0.317	0.269 0.323	0.282 0.329	0.293 0.346	0.288 0.344	0.281 0.342	0.274 0.329	0.321 0.351	0.299 0.337	0.287 0.322
	720	0.327 0.371	0.341 0.381	0.335 0.378	0.363 0.387	0.373 0.387	0.398 0.397	0.378 0.397	0.397 0.421	0.362 0.385	0.408 0.403	0.368 0.393	0.380 0.375
	Avg	0.234 0.300	0.243 0.310	0.239 0.306	0.254 0.314	0.265 0.315	0.277 0.329	0.272 0.331	0.267 0.334	0.255 0.315	0.291 0.333	0.264 0.313	0.264 0.308
Weather	96	0.117 0.204	0.129 0.222	0.126 0.224	0.131 0.224	0.139 0.238	0.196 0.287	0.132 0.227	0.153 0.237	0.129 0.222	0.168 0.272	0.133 0.217	0.134 0.227
	192	0.139 0.230	0.147 0.241	0.148 0.235	0.152 0.241	0.153 0.251	0.199 0.291	0.153 0.249	0.152 0.249	0.147 0.240	0.184 0.289	0.144 0.229	0.145 0.232
	336	0.150 0.248	0.162 0.258	0.161 0.252	0.160 0.248	0.169 0.266	0.214 0.305	0.167 0.262	0.169 0.267	0.163 0.259	0.198 0.300	0.160 0.242	0.166 0.255
	720	0.186 0.279	0.199 0.288	0.196 0.282	0.192 0.298	0.206 0.297	0.254 0.335	0.254 0.335	0.233 0.344	0.197 0.290	0.220 0.320	0.208 0.304	0.189 0.279
Traffic	Avg	0.148 0.240	0.159 0.253	0.158 0.248	0.159 0.253	0.167 0.263	0.216 0.316	0.210 0.304	0.268 0.274	0.159 0.253	0.193 0.295	0.161 0.248	0.158 0.248
	96	0.140 0.188	0.153 0.203	0.146 0.196	0.147 0.201	0.162 0.212	0.171 0.214	0.163 0.211	0.152 0.237	0.149 0.198	0.172 0.220	0.153 0.199	0.158 0.202
	192	0.185 0.231	0.201 0.250	0.190 0.240	0.189 0.234	0.204 0.248	0.217 0.254	0.205 0.250	0.220 0.282	0.194 0.241	0.219 0.261	0.196 0.239	0.202 0.238
	336	0.230 0.270	0.256 0.293	0.240 0.280	0.262 0.279	0.254 0.286	0.274 0.293	0.254 0.289	0.265 0.319	0.245 0.282	0.280 0.306	0.230 0.258	0.253 0.283
720	Avg	0.305 0.318	0.331 0.345	0.312 0.330	0.304 0.316	0.326 0.337	0.329 0.340	0.329 0.340	0.340 0.362	0.314 0.334	0.365 0.359	0.303 0.326	0.332 0.335
	96	0.215 0.251	0.235 0.273	0.222 0.262	0.225 0.258	0.236 0.271	0.248 0.275	0.238 0.273	0.240 0.300	0.225 0.264	0.259 0.286	0.220 0.256	0.236 0.265
	192	0.330 0.242	0.343 0.248	0.338 0.245	0.362 0.248	0.388 0.282	0.401 0.291	0.351 0.257	0.410 0.282	0.360 0.249	0.593 0.321	0.384 0.250	0.391 0.262
	336	0.352 0.250	0.362 0.257	0.360 0.251	0.374 0.247	0.407 0.290	0.432 0.298	0.364 0.265	0.423 0.287	0.379 0.256	0.617 0.333	0.393 0.253	0.407 0.265
720	Avg	0.364 0.261	0.374 0.264	0.370 0.260	0.388 0.264	0.414 0.294	0.429 0.304	0.379 0.272	0.434 0.295	0.391 0.264	0.620 0.329	0.409 0.260	0.422 0.276

Table 8: Long-term forecasting results. Most results of other methods derive from [149] and [167]. Results not reported are obtained by running each method’s source code; the look-back window is selected from {96, 336, 512, 672} to report the best results.